Mon. Not. R. Astron. Soc. **000**, 000–000 (0000) Printed 2 December 2015 (MN LATEX style file v2.2)

The young radio lobe of 3C 84: inferred gas properties in the central 10 parsec

Yutaka Fujita[1⋆], Nozomu Kawakatu[2], Isaac Shlosman[3,1], and Hirotaka Ito[4]
[1] *Department of Earth and Space Science, Graduate School of Science, Osaka University, 1-1 Machikaneyama-cho, Toyonaka, Osaka 560-0043, Japan*
[2] *Faculty of Natural Sciences, National Institute of Technology, Kure College, 2-2-11 Agaminami, Kure, Hiroshima, 737-8506, Japan*
[3] *Department of Physics and Astronomy, University of Kentucky, Lexington, KY 40506-0055, USA*
[4] *Astrophysical Big Bang Laboratory, RIKEN, Saitama 351-0198, Japan*

arXiv:1510.08460v2 [astro-ph.HE] 1 Dec 2015

Accepted 0000 December 00. Received 0000 December 00; in original form 0000 October 00

ABSTRACT
We analyse the environment of the supermassive black hole (SMBH) in the centre of a massive elliptical galaxy NGC 1275 in the Perseus cluster, hosting the radio source 3C 84. We focus on the young radio lobe observed inside the estimated Bondi accretion radius. We discuss the momentum balance between the jet associated with the lobe and the surrounding gas. The results are compared with the proper motion of the radio lobe obtained with the very long baseline interferometry. We find that under assumption of a high-density environment ($\gtrsim 100\,\mathrm{cm}^{-3}$), the jet power must be comparable to the Eddington luminosity — this is clearly inconsistent with the current moderate activity of 3C 84, which indicates instead that the jet is expanding in a very low density region ($\lesssim 1\,\mathrm{cm}^{-3}$), along the rotation axis of the accretion flow. The power required for the jet to expand in the low-density environment is comparable to the past average jet power estimated from the X-ray observations. We estimate the classical Bondi accretion rate, assuming that (1) gas accretion is spherically symmetric, (2) accretion is associated with the jet environment, and (3) the medium surrounding the jet is representative of the properties of the dominant accreting gas. We find that Bondi accretion is inconsistent with the estimated jet power. This means that either accretion of the cold gas in the NGC 1275 is more efficient than that of the hot gas, or the jets are powered by the SMBH spin.

Key words: accretion, accretion discs — galaxies: active — galaxies: individual: 3C84 (NGC 1275) — galaxies: jets — X-rays: galaxies.

1 INTRODUCTION

Gravitational potential energy of the accreting gas is converted into radiation, and into kinetic and thermal energies in accretion flows onto supermassive black holes (SMBHs). This is the essence of the active galactic nuclei (AGN) phenomenon. Such activities include strong outflows, sometimes associated with relativistic jets, which exert a great impact on the surroundings (e.g. Begelman & Cioffi 1989). Most of the activities occur in the vicinity of the SMBH, which makes it difficult to resolve.

The compact radio source 3C 84, hosted by the Seyfert galaxy NGC 1275, may be an exceptional AGN, because it is located at the centre of the nearby cluster (Perseus; $z = 0.018$). Very long baseline interferometry (VLBI) observations have revealed that 3C 84 exhibits complicated radio structure on parsec scales. It consists of a bright core with a flat spectrum and a mushroom-like southern lobe with a steep spectrum (Venturi et al. 1993; Walker, Romney, & Benson 1994; Asada et al. 2006, see Fig. 1). The proper motion of the southern lobe ($\sim$ 0.3 mas yr^{-1}) have also been noticed in radio observations (Romney et al. 1982; Walker, Romney, & Benson 1994). While the synchrotron emission from relativistic electrons provides us with information on the detailed structure of the radio lobe and the jet forming this lobe, not much is known about the thermal hot gas surrounding them. This is because even with the superb resolution of *Chandra*, the gas morphology within ~ 5 kpc from the SMBH remains unresolved (Fabian et al. 2006, but see Wong et al. 2014 for NGC 3115). The hot gas in this region gradually accretes on to the SMBH and fuels the AGN. In particular, the form of accretion in the immediate vicinity of the SMBH (say within the Bondi accretion radius) can determine the energy con-

⋆ E-mail: fujita@vega.ess.sci.osaka-u.ac.jp

© 0000 RAS

version to the radiative, kinetic, and thermal energies (e.g. Yuan & Narayan 2014). Thus, it is very important to know the state of the hot gas there, because it determines the gas accretion on to the SMBH.

Some radio observations have hinted at the existence of a dense gas on scales of several parsecs. O'Dea, Dent, & Balonek (1984) argued about the presence of a thermal gas of a density $\sim$ 2000 cm^{-3} and of a temperature 10^4 K surrounding the core of 3C 84. This is based on an exponential cutoff at the low-frequency end of the compact core spectrum as well as the very low polarization at radio frequencies. Successive radio observations showed that the absorption is spatially biased and that the dense gas may be distributed in a form of a disc (Vermeulen, Readhead, & Backer 1994; Walker, Romney, & Benson 1994). This kind of dense gas has been observed in other galactic cores (e.g. Kameno et al. 2000; Pihlström, Conway, & Vermeulen 2003). Although detection of absorption can constrain the properties of cold gas in the galactic centre, such a gas probably occupies only a small volume. Faraday rotation may also provide a clue on the gas density (Plambeck et al. 2014). However, it is an integrated quantity along the line-of-sight and depends on the properties of magnetic fields.

In this paper, we explore the properties of hot gas surrounding the SMBH in NGC 1275 using VLBI observations of the radio lobe, estimated to lie within the Bondi radius. We focus on the fact that the evolution of the jet associated with the lobe depends strongly on the environment as well as on the jet power which feeds the lobe. Thus, we discuss the momentum balance between the jet and the surrounding gas, compare the results with the observed proper motion of the lobe, and derive information about the environment. The jet power analysis is based on the kinematics of the young lobe, which differs from the previous approach based on radio power (Rawlings & Saunders 1991; Godfrey & Shabala 2013).

The redshift of the NGC 1275 ($z = 0.018$) corresponds to an angular diameter distance of 75.5 Mpc and an angular scale of 0.366 pc mas^{-1} for the Hubble constant of 70 km s^{-1}Mpc^{-1}.

2 MODELS

In this section, we explain our model for the evolution of the jets injected by the SMBH at the centre of NGC 1275. The jet is included in the young radio lobe (Fig. 1).

2.1 Young Radio Lobe at the Centre of NGC 1275

First, we summarize properties of the young radio lobe associated with 3C 84 at the centre of NGC 1275; they are used as input parameters in our models. Asada et al. (2006) performed *VLBI Space Observatory Programme (VSOP)* observations of 3C 84 and revealed the details of the the radio structure. In Fig. 1, the core is at the galactic centre and the brightest spot in the southern lobe is the hotspot at the end of the jet. The northern counter lobe is dark. Asada et al. (2006) estimated the inclination angle of the jets from the apparent distances to the northern and southern radio lobes from the galactic centre and found that it is $\theta = 53^\circ.1 \pm 7^\circ.7$.

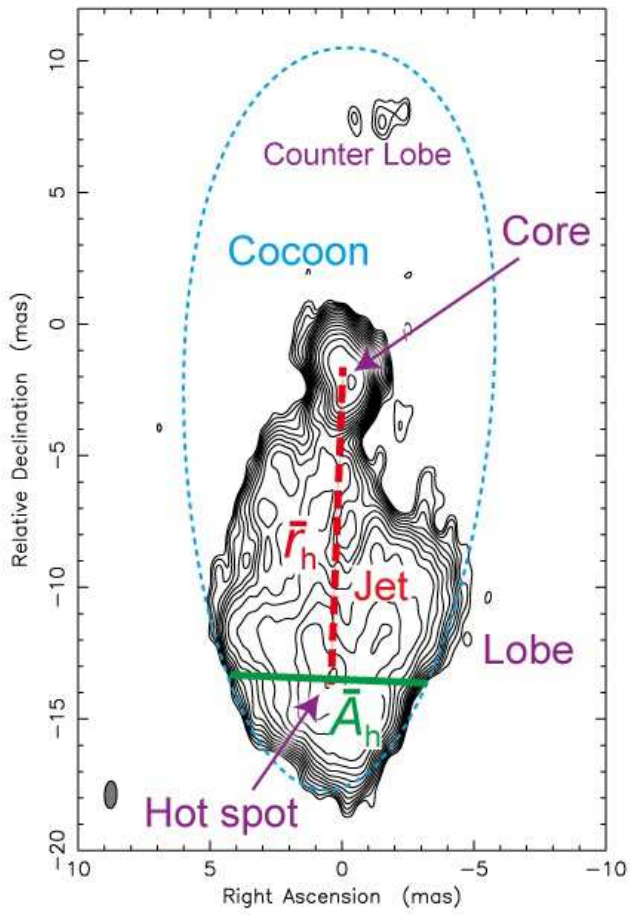

Figure 1. *VSOP* radio image of 3C 84 in 2001 (fig. 3 of Asada et al. 2006). We evaluated the distance from the galactic centre to the hotspot, $r_{\rm h0}$, and the cross-section area of the cocoon head, $A_{\rm h0}$, from the lengths of the thick dashed line and thick solid line, respectively (see text). The thick dashed line also indicates the position of the possible jet. The estimated cocoon containing the radio lobes is shown by the dotted line.

They observed 3C 84 on 1998 August 25 at 4.916 GHz and on 2001 August 21 at 4.865 GHz. We refer to the 'current' time ($t = t_{\rm age}$) as the time at the second observation (2001 August 21). Asada et al. (2006) detected the motion of the hotspot between the two observations and found that its apparent velocity is $v_{\rm a0} = (0.32 \pm 0.08)c$ towards the south for our Hubble constant. Thus, the actual velocity is given by

$$\frac{v_{\rm h0}}{c} = \frac{v_{\rm a0}}{c \sin\theta + v_{\rm a0}\cos\theta} \approx 0.32\,, \qquad (1)$$

where the quantity with the subscript zero is measured at $t = t_{\rm age}$, so $v_{\rm h0} = v_{\rm h}(t_{\rm age})$, where $v_{\rm h}(t)$ is the velocity of the hotspot at time t. We expect that the radio lobes are included in a cocoon that is filled with cosmic rays injected by the jets. The configuration of the jet and the cocoon is shown in Fig. 1 (see also fig. 1 of Kawakatu & Kino 2006 or fig. 1 of Ito et al. 2008). The velocity of the hotspot, $v_{\rm h}(t)$, is also the advance velocity of the cocoon head.

In Fig. 1, the apparent distance between the galactic centre and the hotspot is 12.2 mas (thick dashed line). Considering the inclination angle of the jet θ, the actual distance is $r_{\rm h0} \approx 5.6$ pc. The diameter of the radio lobe at the hotspot

is 7.5 mas (thick solid line in Fig. 1). Thus, the cross-section area of cocoon head is $A_{\rm h0} = \pi(7.5/2)^2$ mas^2 = 5.9 pc^2.

We note here that there are some uncertainties in the radio observations. Asada et al. (2006) estimated the expansion velocity, $v_{\rm a0} = 0.32\,c$ from the apparent motion of the peak of the lobe surface brightness, by measuring the distance from the core. Although the core has two components, Asada et al. (2006) used the position of the resolved most northern component as the reference point (see their fig. 3). Thus, the ambiguity of the core position is expected to be small. On the other hand, the motion of the peak may reflect the pattern velocity of the lobe, and not the physical expansion velocity. Moreover, the *instantaneous* hotspot may not be moving with the working surface represented by $A_{\rm h}$. If there is an error of a factor of 2 in the apparent velocity of the hotspot ($v_{\rm a0}$), which is probably too large, it will cause an error of a factor of 3 or 4 in the jet power (equations 1 and 7 below). Lastly, Asada et al. (2006) obtained the inclination angle of the jet, $\theta = 53.1^\circ \pm 7.7^\circ$, from the ratio of the distances from the galaxy centre to the south and north lobes. However, it has been indicated that free–free absorption can affect the northern lobe (Walker & Anantharamaiah 2003). Hence, if the absorption is highly inhomogeneous, it may affect the estimated distances to the lobes. We also note that Lister et al. (2009) took a different approach, by observing the apparent motions of both southern and northern lobes by fitting them with a Gaussian model, and by determining the inclination angle of the jets to be $\theta \sim 11^\circ$ from the velocities of the southern lobe ($\sim 0.31\,c$) and the northern lobe ($\sim 0.08\,c$). The former is consistent with Asada et al. (2006). The Gaussian fitting may be less sensitive to the pattern change in the lobes, although the complex core component may still have an influence on the measurement (Lister et al. 2009). We have confirmed that our conclusions about the jet power is almost the same (within a factor of a few), even if we adopt $\theta = 11^\circ$ instead of $53.1^\circ \pm 7.7^\circ$. However, this value θ has a problem with the age of the jet (see Section 3). We also note that recent *Fermi* observations have shown that the inclination angle of the jets should be $\theta \sim 25^\circ$–32° from the gamma-ray spectrum (Abdo et al. 2009). Considering the overall insensitivity of the results to the inclination angle, we adopt $\theta = 53^\circ.1$ from now on.

2.2 Ambient Gas Profile

In our discussion of the evolution of the jet, including the radio lobe, we need to specify the properties of the surrounding gas. *Chandra* observations have shown that the electron number density of the hot gas increases and the temperature decreases towards the galactic centre, and they reach $n_{\rm e} \sim 0.1$ cm^{-3} and $T \sim 3$ keV, respectively, at $r \sim 10$ kpc from the centre (e.g. Fabian et al. 2006; Rafferty et al. 2006; Graham, Fabian, & Sanders 2008, see Fig. 2). At $r \sim 5$–10 kpc, the hot gas is strongly affected by the X-ray cavities created by past AGN activities, and the density is $n_{\rm e} \sim 0.05$ cm^{-3}, and the temperature is $T \sim 3$ keV (Fabian et al. 2006, see Fig. 2). There is no information on the gas for $r \lesssim 5$ kpc.

Assuming that the gas temperature around the galactic centre ($r \lesssim 10$ kpc) is $T = 3$ keV and the mass of the central black hole is $M_\bullet = 8 \times 10^8\,M_\odot$ (Scharwächter et al. 2013), the Bondi radius is

$$r_{\rm B} = \frac{2GM_\bullet}{c_{\rm s}^2} = 8.6\ {\rm pc}\,, \qquad (2)$$

where $c_{\rm s}$ is the sound velocity. This radius is comparable to the current length of the jet ($r_{\rm h0} \sim 5.6$ pc, Section 2.1). Since $r_{\rm B}$ is much smaller than the innermost radius for the X-ray observations ($r \sim 5$–10 kpc), we extrapolate the observed gas density profiles towards $r_{\rm B}$ using a power law:

$$n_{\rm e}(r) = n_{\rm e,obs}\left(\frac{r}{r_{\rm obs}}\right)^{-b}\,, \qquad (3)$$

for $r_{\rm B} < r < r_{\rm obs} = 10$ kpc. We assume that the gas distribution is spherically symmetric for simplicity. The density $n_{\rm e,obs}$ and the index b is the parameters for which we consider two extreme cases. In the first model (model EX), we just extrapolate the density profile for $r \gtrsim 10$ kpc (Fig. 2), and we set $n_{\rm e,obs} = 0.1\,{\rm cm}^{-3}$ and $b = 1$. In this case, the gas density at $r_{\rm B}$ is $n_{\rm e,B} = 116$ cm^{-3}. In the second model (model FL), we assume that a flat density profile, and we set $n_{\rm e,obs} = n_{\rm e,B} = 0.05$ cm^{-3} and $b = 0$ (Fig. 2). This may reflect a case where thermal instability of the gas is effective and most of the hot gas turns into cold gas (Barai, Proga, & Nagamine 2012; Gaspari, Ruszkowski, & Sharma 2012; McCourt et al. 2012; Sharma et al. 2012; Guo & Mathews 2014; Meece, O'Shea, & Voit 2015). Since simulations show $b > 0$ (e.g. Gaspari, Ruszkowski, & Oh 2013), we expect that $b = 0$ is a lower limit. While the remaining hot gas occupies most of the volume, the density is significantly reduced around the centre.

We assume that the density profile for $r < r_{\rm B}$ is given by another power law:

$$n_{\rm e}(r) = n_{\rm e,B}\left(\frac{r}{r_{\rm B}}\right)^{-\alpha}\,, \qquad (4)$$

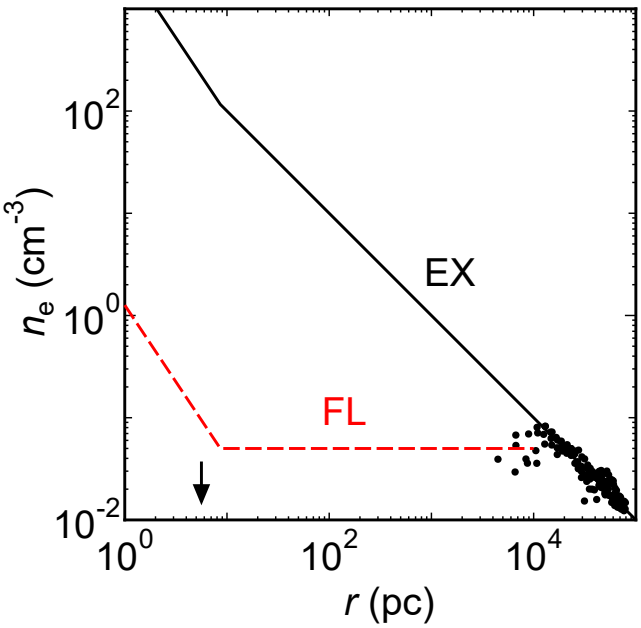

Figure 2. Assumed density and temperature profiles. Dots are the *Chandra* observations (Fabian et al. 2006). The arrow shows the length of the jet ($r_{\rm h0}$).

where $n_{\rm e,B} = n_{\rm e}(r_{\rm B})$, and α is the parameter. In this region, the gas distribution should be strongly affected by the SMBH. If the gas falls nearly freely into the SMBH, the infall velocity is $v \propto r^{-1/2}$ from the energy conservation, and α should be 1.5, from the mass conservation. This profile approximates the one for the classical Bondi accretion (Bondi 1952). On the other hand, $0.5 \leqslant \alpha \leqslant 1.5$ was suggested by Blandford & Begelman (1999) in the context of advection-dominated inflow-outflow solutions (ADIOS). Moreover, recent numerical simulations of a gravitational collapse in the presence of the gas cooling have shown that the slope should be $0 \leqslant \alpha \leqslant 1.5$ (e.g., Choi, Shlosman, & Begelman 2013, 2015). We have confirmed that the results are not sensitive to the value of α as long as $0 \lesssim \alpha \lesssim 1.5$. Thus, we assume $\alpha = 1.5$ from now on.

2.3 Evolution of the Jet

The momentum balance along the jet is given by

$$\frac{L_{\rm j}}{v_{\rm j}} = \rho(r_{\rm h}) v_{\rm h}(t)^2 A_{\rm h}(t) \, , \tag{5}$$

where $L_{\rm j}$ is the kinematic power of the jet, $v_{\rm j}$ is the velocity of the jet, $r_{\rm h}$ is the distance to the hotspot from the galactic centre, and $A_{\rm h}$ is the cross-section area of the cocoon head. We assume that $L_{\rm j}$ is time-independent and $v_{\rm j} = c$. We also assume that the opening angle of the cocoon head, $\theta_{\rm h} = \arctan(A_{\rm h}^{1/2}/(\pi^{1/2} r_{\rm h}))$, is constant in time. Since the jet lies within the Bondi radius at present ($r_{\rm h0} < r_{\rm B}$), the density profile of the ambient gas is given by equation (4) and can be rewritten as

$$\rho(r) = \rho_{\rm B} (r/r_{\rm B})^{-\alpha} \, . \tag{6}$$

From equations (5) and (6), we obtain

$$L_{\rm j} = \rho(r_{\rm h0}) c v_{\rm h0}^2 A_{\rm h0} \, , \tag{7}$$

and

$$t_{\rm age} = \frac{2 r_{\rm h0}}{4 - \alpha} \left(\frac{r_{\rm h0}}{r_{\rm B}} \right)^{-\alpha/2} \left(\frac{L_{\rm j}}{\rho_{\rm B} c A_{\rm h0}} \right)^{-1/2} \, . \tag{8}$$

3 RESULTS

We take $r_{\rm h0} = 5.6$ pc, $A_{\rm h0} = 5.9\,{\rm pc}^2$, and $v_{\rm h0} = 0.32c$ (Section 2.1). From equations (4), (7), and (8), we obtain $n_{\rm e}(r_{\rm h0})$, $L_{\rm j}$ and $t_{\rm age}$, respectively. Our results are summarized in Table 1. Since there are two jets (north and south), the total jet power is represented by $2L_{\rm j}$. The power decreases as the ambient gas density at $r = r_{\rm h0}$ or $n_{\rm e}(r_{\rm h0})$ decreases, and thus model EX gives the higher power (Table 1). This is because a larger density of the surrounding gas requires a larger jet power to excavate for a given current advance speed of the jet (equations 6–8).

The age of the jet $t_{\rm age}$ does not depend on $n_{\rm e}(r_{\rm h0})$ for a given α and the fixed $v_{\rm h0}$. Again, this is because a larger ambient density requires a larger a jet power to excavate; $L_{\rm j}/\rho_{\rm B}$ does not depend on $\rho_{\rm B}$ in equation (8) (see also equations 6 and 7). Since $t = t_{\rm age}$ corresponds to 2001, the jet was born in 1955. Observations have indicated that an outburst started in 1959 (e.g. Nesterov, Lyuty, & Valtaoja 1995). Our model is almost consistent with the idea that this outburst corresponds to the formation of the radio lobes. We note that regardless of the density profile (EX or FL), models with the inclination angle of $\theta = 11^\circ$ (Section 2.1) predict that the jet was born before 1940, which is not consistent with the observed outburst in 1959.

Next, we compare the obtained jet power with other quantities associated with the SMBH and AGN in this galaxy. The Eddington luminosity is given by

$$L_{\rm Edd} = 1.26 \times 10^{38} \left(\frac{M_\bullet}{M_\odot} \right) \, {\rm erg \, s^{-1}} \, . \tag{9}$$

Since gas kinematics suggests $M_\bullet = 8 \times 10^8 \, M_\odot$ (Scharwächter et al. 2013) for NGC 1275, the luminosity is $L_{\rm Edd} = 1.0 \times 10^{47} \, {\rm erg \, s^{-1}}$. In Table 1, we present $2L_{\rm j}/L_{\rm Edd}$. Model EX predicts that the ratio is close to one. However, such a high ratio is accepted only for extremely active AGNs, which radiate efficiently as QSOs. It is not likely to be realized for moderate AGNs, including 3C 84 (e.g. Yuan & Narayan 2014). In fact, the X-ray luminosity of 3C 84 is $\sim 10^{43} \, {\rm erg \, s^{-1}}$, much smaller than $L_{\rm Edd}$ (Donato, Sambruna, & Gliozzi 2004).

Another interesting quantity is the cavity power $P_{\rm cav}$, which is required to inflate X-ray cavities observed around an AGN. The cavities are thought to be the relics of cocoons. In the case of NGC 1275, cavities are located at $r \gtrsim 1$ kpc from the centre (Fabian et al. 2006), and the volume $V_{\rm cav}$ can be estimated from their sizes. The total energy required to create a cavity is equal to its enthalpy and it is given by

$$E_{\rm cav} = \frac{\gamma_{\rm c}}{\gamma_{\rm c} - 1} p_{\rm gas} V_{\rm cav} \, , \tag{10}$$

where $\gamma_{\rm c} = 4/3$ is the adiabatic index for relativistic gas, and $p_{\rm gas}$ is the pressure of the gas surrounding the cavities, which can be estimated from X-ray observations. The cavity power is defined by

$$P_{\rm cav} = E_{\rm cav}/t_{\rm burst} \, , \tag{11}$$

where $t_{\rm burst}$ is the average time between outbursts of the AGN. Rafferty et al. (2006) estimated that the cavity power with NGC 1275 is $P_{\rm cav} \sim 1.5 \times 10^{44} \, {\rm ergs^{-1}}$, which may represent the average jet power over the period of $t_{\rm burst} \sim 10^7$ yr. In Table 1, we provide the ratio $2L_{\rm j}/P_{\rm cav}$. For model EX, this ratio is much larger than unity, which means that the current jet power exceeds substantially the past average. Since the probability to observe the jet activity is $\sim (2L_{\rm j}/P_{\rm cav})^{-1}$, it is unlikely that such activity is actually occurring at present. On the other hand, the same ratio in model FL is close to unity (Table 1), which means that the current jet activity is not very different from the past average. Note, that the energy inside the cavity or the cocoon could also be estimated by means of the minimum-energy condition. Using this condition, Nagai et al. (2009) estimated that the jet power is $\sim 10^{42} \, {\rm erg \, s^{-1}}$, which is more than one orders of magnitude smaller than the predictions of model FL (Table 1). However, it has been indicated that this condition is not met for NGC 1275, and that the cavities may contain hidden relativistic particles, such as protons (Fabian et al. 2002; Nagai et al. 2009).

The Bondi accretion rate is given by

$$\dot{M}_{\rm B} = (\pi/4) c_{\rm s,0} \rho_{\rm B} r_{\rm B}^2 \, , \tag{12}$$

(Bondi 1952). Assuming efficiency of 10%, the maximal

Table 1. Results

Model	$n_{\rm e}(r_B)$ ($\rm cm^{-3}$)	α	$n_{\rm e}(r_{\rm h0})$ ($\rm cm^{-3}$)	$t_{\rm age}$ (yr)	$2L_{\rm j}$ ($\rm erg\,s^{-1}$)	$2L_{\rm j}/L_{\rm Edd}$	$2L_{\rm j}/P_{\rm cav}$	$P_{\rm B}$ ($\rm erg\,s^{-1}$)	$2L_{\rm j}/P_{\rm B}$
EX	116	1.5	222	46	1.3×10^{47}	1.3	869	9.8×10^{44}	133
FL	0.05	1.5	0.096	46	5.6×10^{43}	5.6×10^{-4}	0.37	4.2×10^{41}	133

Note — Column (1): Model name. Column (2) Gas density at the Bondi radius. Column (3): Index of gas profile within the Bondi radius. Column (4): Gas density at the tip of the jet. Column (5): Jet age. Column (6): Jet power. Column (7): Ratio of jet power to Eddington luminosity. Column (8): Ratio of jet power to cavity power. Column (9) Bondi accretion power. Column (10): Ratio to jet power to Bondi accretion power.

power released from the vicinity of the SMBH by the Bondi accretion is

$$P_{\rm B} = 0.1\dot{M}_{\rm B}c^2\,. \tag{13}$$

For reference reasons only, we have calculated the ratio $2L_{\rm j}/P_{\rm B}$ for all the models, using the idealized spherical Bondi accretion rate.

The ratio $2L_{\rm j}/P_{\rm B}$ depends on the accreting gas properties, i.e., on its density profile, and its temperature. Thus, models EX and FL, for a given α, result in the same values of $2L_{\rm j}/P_{\rm B} \gg 1$. This means that the characteristic Bondi accretion rate cannot provide enough power to sustain the observed jets regardless of the gas properties around the Bondi radius. We emphasize that this argument can be applied when the accretion is spherically symmetric, and the jet environment and accretion are correlated.

We have assumed that the jet is interacting with the hot gas in NGC 1275. However, the central region of the galaxy is very complicated and the gas may be multiphase. For example, the jet may be interacting with dense cool gas $\gtrsim 1000\,\rm cm^{-3}$ mentioned in Section 1. In this case, however, the jet power must be even larger than that for model EX (Table 1) in order to be consistent with the current jet velocity. Such an extreme jet power ($2L_{\rm j}/L_{\rm Edd} \gg 1$) is very unlikely. On the other hand, the lobe may be expanding into an existing larger scale radio lobe, in which gas density is much smaller than that in model FL. If this is the case, the jet power and $2L_{\rm j}/P_{\rm cav}$ are also much smaller than those in model FL (Table 1). This means that the current jet activity is much weaker than the time average.

In summary, the ratios $2L_{\rm j}/L_{\rm Edd}$ and $2L_{\rm j}/P_{\rm cav}$ show that the lower density model (FL) is preferable to the higher density model (EX) in terms of the current and past moderate activities of the AGN. The classical Bondi accretion model can be rejected, because it cannot provide enough jet power regardless of the ambient gas density.

4 DISCUSSION AND CONCLUSIONS

The results in Section 3 indicate that the gas density around the cocoon is likely to be $\lesssim 1\,\rm cm^{-3}$ (model FL). This low density may result from thermal instabilities, as we mentioned in Section 2.2. Another possibility is that the hot gas is distributed highly anisotropically, and its density in the direction of the jets is substantially smaller than in other directions, perhaps because previous generations of jets have drilled tunnels. The jet which has been analysed here is expanding nearly freely through low-density environment (model FL) at present. Since this reduces energy loss of the jet during the expansion against the ambient gas, it may contribute to the efficient energy transport from the jets to the intracluster medium, and contribute to the suppression of a massive cooling flow (e.g. Fujita & Ohira 2013).

On the other hand, some radio observations have detected absorbing material with a density of $> 1000\,\rm cm^{-3}$ on the scale of several parsecs (O'Dea, Dent, & Balonek 1984). A possible solution is that the dense gas forms a cold disc around the SMBH, and the jets are launched perpendicular to the disc. Walker & Anantharamaiah (2003) indicated the northern counter lobe shown in Fig. 1 is absorbed. This suggests that the size of the disc is at least comparable to the apparent distance to the northern lobe (~ 3 pc).

Our results show that the classical Bondi accretion cannot provide enough power to sustain the observed jets. Addition of angular momentum to the accreting gas will not improve the situation in any substantial way, because while the gas density decreases along the the rotation axis (which is the direction of jet propagation), the gas accretion rate to the SMBH decreases as well. The gas will be diverted away from the rotation axis towards the equatorial plane and may accumulate there (e.g. Proga & Begelman 2003; Krumholz, McKee, & Klein 2005). The fate of this gas is outside the scope of this paper, but it can be either converted to stars, expelled in a wind, or be accreted by the SMBH in the disc accretion mode.

This indicates that it is the cold gas, rather than the hot gas, that fuels the SMBH (Shlosman et al. 1989; Pizzolato & Soker 2010; Gaspari, Ruszkowski, & Oh 2013). However, such process requires an efficient mechanism which removes the angular momentum from the gas, such as gravitational (Shlosman et al. 1989, 1990) or magnetic (Blandford & Payne 1982; Emmering, Blandford, & Shlosman 1992) torques. The cold gas can originate in thermal instabilities, and can form a disc around the SMBH. If the disc is turbulent, this would decrease the mass inflow time-scale and correspondingly increase the accretion rate on to the SMBH (Shlosman et al. 1990; Kawakatu & Wada 2008). Alternatively, the jets can be powered by the SMBH spin (Blandford & Znajek 1977). The existence of a cold disc gas can be confirmed by future observations (e.g. ALMA).

In this model, we do not consider relativistic effects in the jet model (Section 2.3). However, they do not significantly affect the results because of the short duration of the relativistic expansion of the jet ($v_{\rm h} \sim c$). Using equations (5) and (6) and the assumption of a constant opening angle, one can obtain $v_{\rm h} \propto t^{(\alpha-2)/(4-\alpha)}$. Thus, the jet expands as $v_{\rm h} \propto t^{-0.2}$ for $\alpha = 1.5$. Therefore, the duration of the relativistic expansion is only $\sim 0.003\,t_{\rm age}$ for a given

$v_{\rm h0} = 0.32\,c$. In fact, the jet evolution (e.g. $r_{\rm h}(t)$) is insensitive to the choice of the start time of the expansion (Ito et al. 2008).

To summarize, we have studied the environment of the young radio lobe observed at $\lesssim 10$ pc from the SMBH at the centre of the galaxy NGC 1275 (or the radio source 3C 84) in the Perseus cluster. The lobe is located inside the estimated Bondi accretion radius. The lobe should be associated with the cocoon created by jet activities in the AGN, and the evolution of the jet should depend on the jet power and the properties of the hot ambient gas.

Using a simple model and comparing it with the proper motion of the lobe obtained through VLBI observations, we constrain the jet power and the environment in the vicinity of the SMBH. We find that a low-density environment $\lesssim 1$ cm^{-3} is more plausible, considering the current and past modest activities of the AGN. This low density hot gas can result from the thermal instabilities in a denser precursor gas. Since the existence of a high-density gas (> 1000 cm^{-3}; O'Dea, Dent, & Balonek 1984; Vermeulen, Readhead, & Backer 1994; Walker, Romney, & Benson 1994) has been indicated in this region, we conjecture that the gas is highly inhomogeneous and it is plausibly forming a disc around the SMBH. Assuming that the accretion is spherically symmetric and is correlated with the gas properties around the jet, and assuming that the gas close to the jet has the properties of the dominant accreting gas, we show that the classical Bondi accretion rate is not consistent with our predicted jet power, and, therefore, can be rejected. The presence of angular momentum in the accreting gas will not improve the situation. A more realistic scenario with the seed angular momentum in the accretion flow makes it plausible that the gas will accumulate in the equatorial plane of the flow, where gravitational or magnetic torques trigger an efficient loss of the angular momentum in the cold gas. This means that either accretion of the cold gas dominates over that of the hot gas, or the jets are powered by the SMBH spin.

ACKNOWLEDGMENTS

We thank the anonymous referee for useful comments. We also thank K. Asada for useful discussion and providing us the image of 3C 84. This work was supported by International Joint Research Promotion Program and Challenge Support Program by Osaka University. This work was also supported by KAKENHI (Y. F.: 15K05080). N. K. acknowledges the financial support of Grant-in-Aid for Young Scientists (B:25800099). I. S. acknowledges partial support from the NSF and STScI. STScI is operated by AURA, Inc., under NASA contract NAS 5-26555. H. I. acknowledges the financial support of Grant-in-Aid for Young Scientists (B:26800159).

REFERENCES

Abdo A. A., et al., 2009, ApJ, 699, 31
Asada K., Kameno S., Shen Z.-Q., Horiuchi S., Gabuzda D. C., Inoue M., 2006, PASJ, 58, 261
Barai P., Proga D., Nagamine K., 2012, MNRAS, 424, 728
Begelman M. C., Cioffi D. F., 1989, ApJ, 345, L21
Blandford R. D., Begelman M. C., 1999, MNRAS, 303, L1
Blandford R. D., Payne D.G, 1982, MNRAS, 199, 883
Blandford R. D., Znajek R. L., 1977, MNRAS, 179, 433
Bondi H., 1952, MNRAS, 112, 195
Choi J.-H., Shlosman I., Begelman M. C., 2013, ApJ, 774, 149
Choi J.-H., Shlosman I., Begelman M. C., 2015, MNRAS, 450, 4411
Donato D., Sambruna R. M., Gliozzi M., 2004, ApJ, 617, 915
Emmering, R.T., Blandford, R.D., Shlosman, I. 1992, ApJ, 385, 460
Fabian A. C., Celotti A., Blundell K. M., Kassim N. E., Perley R. A., 2002, MNRAS, 331, 369
Fabian A. C., Sanders J. S., Taylor G. B., Allen S. W., Crawford C. S., Johnstone R. M., Iwasawa K., 2006, MNRAS, 366, 417
Fujita Y., Ohira Y., 2013, MNRAS, 428, 599
Gaspari M., Ruszkowski M., Oh S. P., 2013, MNRAS, 432, 3401
Gaspari M., Ruszkowski M., Sharma P., 2012, ApJ, 746, 94
Godfrey L. E. H., Shabala S. S., 2013, ApJ, 767, 12
Graham J., Fabian A. C., Sanders J. S., 2008, MNRAS, 386, 278
Guo F., Mathews W. G., 2014, ApJ, 780, 126
Ito H., Kino M., Kawakatu N., Isobe N., Yamada S., 2008, ApJ, 685, 828
Kameno S., Horiuchi S., Shen Z.-Q., Inoue M., Kobayashi H., Hirabayashi H., Murata Y., 2000, PASJ, 52, 209
Kawakatu N., Kino M., 2006, MNRAS, 370, 1513
Kawakatu N., Wada K., 2008, ApJ, 681, 73
Krumholz M. R., McKee C. F., Klein R. I., 2005, ApJ, 618, 757
Lister M. L., et al., 2009, AJ, 138, 1874
McCourt M., Sharma P., Quataert E., Parrish I. J., 2012, MNRAS, 419, 3319
Meece G., O'Shea B., Voit M., 2015, ApJ, 808, 43
Nagai H., Asada K., Doi A., Kameno S., Inoue M., 2009, Astron. Nachtr., 330, 161
Nesterov N. S., Lyuty V. M., Valtaoja E., 1995, A&A, 296, 628
O'Dea C. P., Dent W. A., Balonek T. J., 1984, ApJ, 278, 89
Pihlström Y. M., Conway J. E., Vermeulen R. C., 2003, A&A, 404, 871
Pizzolato F., Soker N., 2010, MNRAS, 408, 961
Plambeck R. L., et al., 2014, ApJ, 797, 66
Proga D., Begelman M. C., 2003, ApJ, 582, 69
Rafferty D. A., McNamara B. R., Nulsen P. E. J., Wise M. W., 2006, ApJ, 652, 216
Rawlings S., Saunders R., 1991, Nature, 349, 138
Romney, J., Alef, W., Pauliny-Toth, I., Preuss, E., & Kellermann, K. 1982, in Heeschen D. M., Wade C. M., eds, Proc. IAU Symp. 97, Extragalactic Radio Sources. Reidel Publishing Co., Dordrecht, p. 291 Proceedings of the Symposium, Albuquerque, NM, August 3-7, 1981. Dordrecht, D. Reidel Publishing Co., 97, 291
Scharwächter J., McGregor P. J., Dopita M. A., Beck T. L., 2013, MNRAS, 429, 2315
Sharma P., McCourt M., Quataert E., Parrish I. J., 2012,

MNRAS, 420, 3174
Shlosman, I., Begelman, M.C., Frenk, J., 1990, Nature, 345, 679
Shlosman, I., Frenk, J., Begelman, M.C., 1989, Nature, 338, 45
Venturi T., Readhead A. C. S., Marr J. M., Backer D. C., 1993, ApJ, 411, 552
Vermeulen R. C., Readhead A. C. S., Backer D. C., 1994, ApJ, 430, L41
Walker R. C., Anantharamaiah K. R., 2003, AJ, 125, 1756
Walker R. C., Romney J. D., Benson J. M., 1994, ApJ, 430, L45
Wong K.-W., Irwin J. A., Shcherbakov R. V., Yukita M., Million E. T., Bregman J. N., 2014, ApJ, 780, 9
Yuan F., Narayan R., 2014, ARA&A, 52, 529